# Robust Model-Based Boundary Cue Generation for Cell Image Interpretation[1]

P. Zhou and D. Pycock
School of Electronic and Electrical Engineering
The University of Birmingham
Email: [P.Zhou, D.Pycock]@bham.ac.uk

**Abstract**

In model based image interpretation the cue generation process must be robust; i.e. able to generate appropriate cues for wide variety of objects. In this work we describe a model-based approach to cue generation and demonstrate its operation on both synthetic test data and natural images of epithelial cells. Epithelial cells were chosen because their appearance is highly variable. Statistical inference is used to interpret step, ramp and composite grey-level edges where an edge is modelled in terms of the grey-level distributions on each side of the edge. This approach provides a measure of confidence for each edge cue generated. The cue generation process reported here is shown to be more selective than other, previously reported methods that in turn compare favourable with the performance of the Canny operator for cue generation. The cue generation process reported here is also shown to be robust for free laying, touching and overlapping cells when combined with a simple boundary interpretation strategy.

## 1. Introduction

Object boundaries are marked by a discontinuity in the pattern of values in an image. However it is difficult to give a definition of grey-level pattern discontinuity that is valid in all situations. Many low-level procedures for boundary detection incorporating particular discontinuity criteria have been proposed. One of the most well know spatial gradient edge detection procedures is the Canny operator[2]. With the Canny operator grey-level discontinuities are estimated by computing the change in grey-level value between regions in an image that span a grey-level edge. Canny describes how the size and orientation of these regions affects the performance of the edge detection process and defines a procedure for determining their size and orientation. The principal limitation of the Canny operator and of many other spatial gradient algorithms is their inability to select support regions and edges that are appropriate to the scale and structure of the object to which that edge might belong. This is a fundamental limitation that arises from the use of grey-level difference criteria in isolation. If spatial smoothing is to be used then the extent of that smoothing should be conditioned by the structure of the image. The scale of smoothing that is appropriate to identify the outline of an object will also depend on the proximity of other objects and will vary for the interpretation of any one object. It is desirable to either merge the results of edge detection using a variety of models or to develop more universal signal

[1]This work is supported by the EPSRC under grant No. GR/G59448.

BMVC 1995 doi:10.5244/C.9.34

When a radial search path is used with regularly shaped objects it can be advantageous to take the average of grey-level values in a direction perpendicular to the search path to increase signal-to-noise ratio. When the shape is irregular or the origin of the search path is "off-centre" with respect to the object, see Figure 2(a), then the grey-level profile will be "blurred" and considerable care is needed to define, in a strategic sense, a suitable search path for locating the grey level edge. The requirement is for a search path that is perpendicular to the boundary in the immediate vicinity of the boundary. A circular search path will meet this requirement for a wide variety of boundary shapes. However the radius of the search path may, in some cases, be critical. To follow the boundary accurately the radius of the circular search path must be small when the boundary curvature is high. However to minimise computational cost the radius of the circular search path should be large. This is satisfactory for straight or near straight sections of boundary. Therefore the selection of a radius for the circular search path is a compromise and an adaptive strategy is required for selecting the radius of curvature so that it can be adapted to suit each section of a boundary.

A piece-wise linear estimate of local curvature is used to guide the choice of radius for the circular search path. Figure 2(b) shows a circular search path, centred on a previously located boundary point, *C*; a new boundary point, *C'*; and the previously located boundary point, E. Using these points the local curvature, *b*, is defined as:

$$b = \frac{C'E}{2R}$$

where: $C'E$ is the distance between $C'$ and $E$
$R$ is the radius of the search path

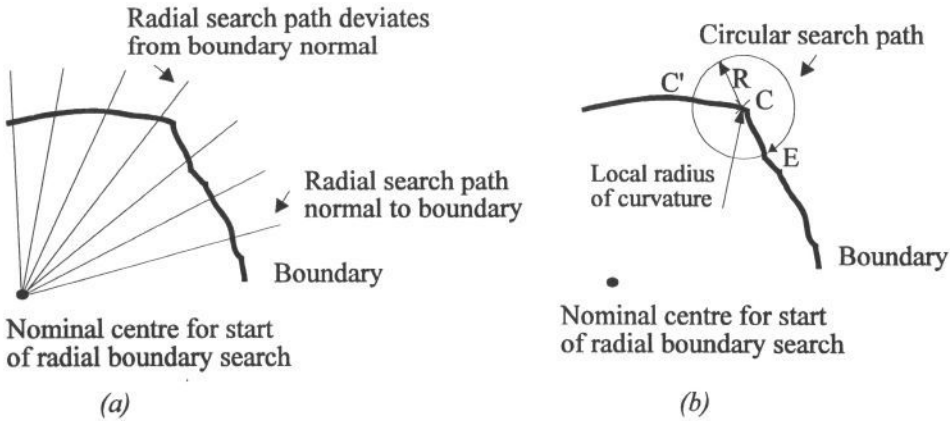


*Figure 2. a) blurring due to radial search path not crossing potential boundary at a perpendicular; b) design of circular search path and estimation of boundary curvature.*

The algorithm used to select the radius of the search path is described in Figure 3. Whilst the radius, *R*, is between the minimum ($R_{min}$) and the maximum ($R_{max}$) permitted value it is adjusted according to the measure of curvature, b. Whilst the value of curvature is less than 0.7 (and the radius is greater than $R_{min}$) the radius of the search

models for low-level processing. Canny discusses the use of alternative grey-level models to describe grey-level edge transitions. However no guidance is given on how to automate the selection of a suitable grey-level edge model.

Models are often used to describe the nature and context of grey-level discontinuities in a flexible way and to guide the application of low-level procedures. The use of a model is often advocated to improve robustness and adaptability in the interpretation of complex scenes. The aim in such approaches is to minimise the computational cost associated with low-level processing and to maximise the benefit of their application. The declarative nature of model-based approaches also simplifies the adaptation of solutions from one problem domain to another. In previous work using maximum likelihood strategies for edge detection it has been assumed that the region being analysed is bimodal[5, 6].

Many simple edge detection procedures provide only an indication of the strength of a particular form of grey-level discontinuity; They do not, for example, provide information that relates the position of edge cues to a structural model or normally provide any measure of confidence. In the work reported here we compare the likelihood that there is no edge and the likelihood that there is an edge using robust principles of statistical inference to provide a measure of edge cue validity.

Most typical epithelial cells, see Figure 1, are "*blob like*"; i.e. they are relatively compact objects. In previous work[1] the "*blob like*" form of muscle fibres in transverse section prompted the use of an implicit geometric model to guide boundary detection. Nominal centres were located and the image sampled along radial lines. This strategy

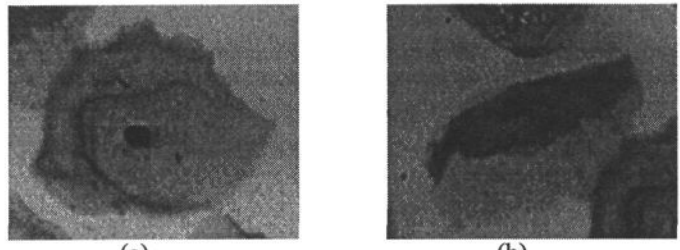

(a) (b)

*Figure 1. Typical epithelial cells showing a dark compact nucleus and a lighter extended region of cytoplasm. a) a typical, compact and mature cell. b) an atypical elongated cell*

was based on the assumption that the objects were almost circular and that the origin from which the radial lines were projected was near the centre of each fibre section. Both assumptions are often over restrictive; especially when considering epithelial cells. In this work we show how the simple addition of a circular search strategy gives improved performance over a radial search strategy in locating boundary points for irregularly shaped objects.

## 2 Boundary Search Strategy

In this section we describe how a search strategy based on circular paths can be used to advantage in locating the potential boundary points on irregular shaped objects.

path is reduced and a new candidate boundary point found. Otherwise the new boundary point $C'$ is accepted. This allows the radius of the search path to be adjusted as the radius of curvature of the boundary changes.

1. Set initial radius of search path, $R$, to a large value ($R_{max}$) and $b$=1.
2. For each initial edge cue:
   - 2.1 If confidence is below some threshold, T, Then:
     - 2.1.1 If (($b > 0.9$) AND ($R < R_{max}$)) Then $R = R \times 1.1$
     - 2.1.2 Perform circular search to locate $C'$
     - 2.1.3 Do
       - 2.1.3.1 Locate intersection with existing boundary, $E$
       - 2.1.3.2 Locate position of new boundary point, $C'$
       - 2.1.3.3 Compute $b = \frac{C'E}{2R}$
       - 2.1.3.4 If ($b < 0.7$) Then $R = R \times b$

       While (($R > R_{min}$) AND ($b < 0.7$))

*Fig. 3 Algorithm for selecting the radius of the circular search path.*

## 3 Grey-Level Edge Model

An observation of grey-level profiles from typical cell images showed that an edge profile may take many forms:

i) an isolated step (see Figure 4a)
ii) an isolated ramp (Figure 4d and 4e)
iii) a step and a ramp in close proximity (Figure 4b and 4c)
iv) two step edges in close proximity
v) two ramp edges in close proximity (Figure 4f)
vi) a barely discernible change (see Figure 4e).

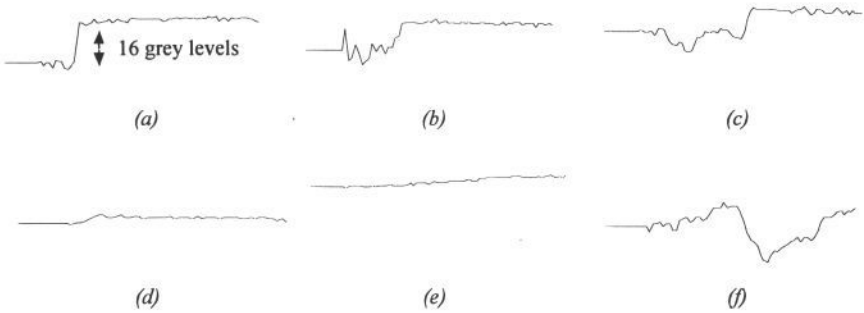


*Figure 4. Example of grey-level profiles across cell cytoplasm boundary. a) isolated step edge, b) and c) step edge and close "noise", d) "distinct" ramp edge, e) barely discernible ramp edge and f) adjacent ramp edges.*

Statistical inference is used to interpret step, ramp and composite grey-level edges where an edge is modelled in terms of the grey-level distributions on each side of the edge. In this interpretation strategy two hypotheses are formulated: i) that there is an edge present and ii) that there is no edge present. A Maximum likelihood strategy[3] is used

to provide evidence for each hypothesis. The likelihood estimates for these hypotheses are combined using statistical inference to provide a well defined measurement that is an indication of confidence that an edge is present.

The likelihood that a data sample, $\bar{x}$, is drawn from a single population, $L_1$ is:

$$L_1\left(\bar{A}|\bar{x}\right) = \prod_{i=1}^{N} p\left(x_i|\bar{A}\right) \qquad \text{(Eq. 1)}$$

where: $x_i$ is the i-th sample of $\bar{x}$
$\bar{x}$ is the grey-level sample vector
$\bar{A}$ is the parameter vector for the grey-level sample
$p(x_i|A)$ is the probability density function of the grey-level sample vector, $\bar{x}$, parameterised by $\bar{A}$.

The likelihood that a data sample, $\bar{x}$, can be divided into two populations is:

$$L_2\left(\bar{A}_o\bar{A}_b|\bar{x}_o\bar{x}_b\right) = \prod_{i=1}^{m} p_o\left(x_i|\bar{A}_o\right) \prod_{j=m+1}^{N} p_b\left(x_j|\bar{A}_b\right) \qquad \text{(Eq. 2)}$$

where: $x_i$ and $x_j$ are samples from $\bar{x}$, the combined sample vector
$\bar{x}_o$ and $\bar{x}_b$ are the sample vectors for the foreground, 'o', and the background, 'b', respectively.
$\bar{A}_o$ and $\bar{A}_b$ are the parameter vectors estimated from $\bar{x}_o$ and $\bar{x}_b$ respectively.
$p_o(x_i|\bar{A}_o)$ and $p_b(x_i|\bar{A}_b)$ are the probability density functions for the sample vectors, $\bar{x}_o$ (and $\bar{x}_b$), parameterised by $\bar{A}_o$ (and $\bar{A}_b$) respectively.

The parameter vectors, $\bar{A}$, $A_o$ and $A_b$, estimated using a Gaussian model and the maximum likelihood strategy as: $\hat{\bar{A}} = [\hat{\mu}, \hat{\sigma}]$, $\hat{\bar{A}}_b = [\hat{\mu}_b, \hat{\sigma}_b]$ and $\hat{\bar{A}}_o = [\hat{\mu}_o, \hat{\sigma}_o]$. Taking the natural logarithm of the ratio $L_2 / L_1$ and substituting for the above population estimates gives the Maximum Likelihood Ratio, MLR:

$$\text{MLR} = \frac{\hat{\sigma}^N}{\hat{\sigma}_o^m \hat{\sigma}_b^{N-m}}$$

## 4 Results

For the purpose of comparison the performance of the maximum-likelihood edge detection operator described here is compared with the standard deviation operator described by Graham and Taylor[4]. Graham and Taylor compared the standard deviation operator with a Canny-based operator and an operator based on a measure of entropy. They compared performance in terms of sensitivity, accuracy of edge localisation and precision of edge localisation using the following measures:

$$\text{Sensitivity, } S = \frac{E(\bar{s}) - E(\bar{n})}{E\left\{\left[\bar{n} - E(\bar{n})\right]^2\right\}}$$

Localisation accuracy, $L_A = E(\overline{d})$

Localisation precision $L_P = \{[\overline{d} - E(\overline{d})]^2\}$

where: $\overline{s}$ is the vector of responses at each true edge
$\overline{n}$ is the vector of responses at each computed edge and
$\overline{d}$ is the vector of distances between each computed edge and the corresponding true edge.

These measures were used to evaluate the performance of the MLR and the SD based edge detection procedures on synthetic images with defined levels of signal to noise ratio. In addition both methods were evaluated using natural images where the pattern of the grey-level edge cannot easily be characterised.

4.1 Synthetic Image Data

These measures were evaluated using synthetic images with a step edge, h, of 1 grey-level value amplitude at a mean grey-level value 128 (in a range 0 to 255). Gaussian distributed noise with a variance of 0.56 to 51 grey-levels was added to this step edge to give signal to noise ratios, h/σ, of: 0.14, 0.20, 0.25, 0.30, 0.35, 0.40, 0.5, 0.6, 0.8, 1.0, 1.2 and 1.33. An area 80 pixels wide by 40 pixels high over the edge in each 256 x 256 synthetic image was scanned to locate the position of the test edge. The size of the test window was also varied from 10 to 50 pixels high and from 20 to 100 pixels wide for both the MLR and the SD operator. The performance of both the MLR and the SD operator improved in a similar manner with increase in size of test window. A typical result is shown in Figure 5 and the complete set of results are summarised in

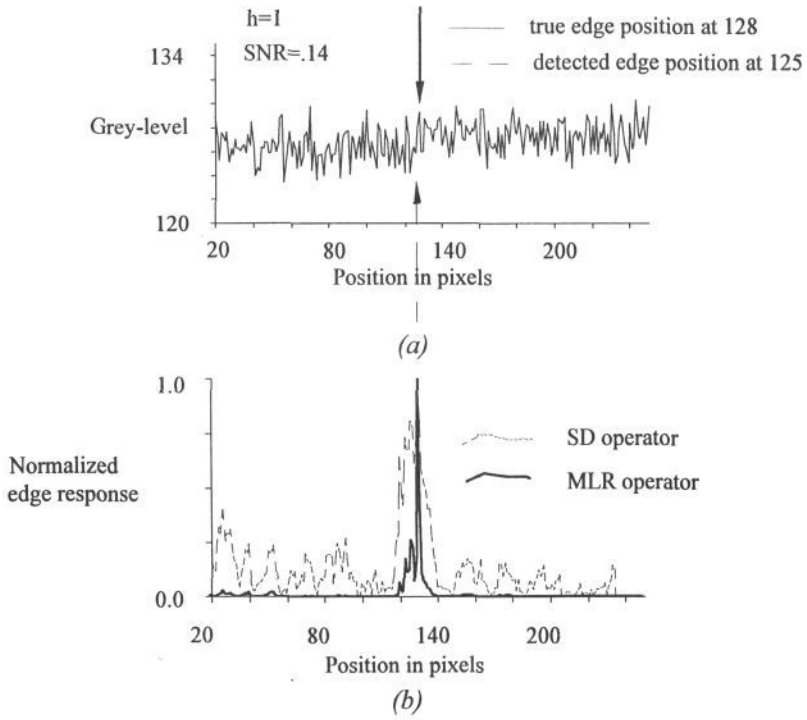


*Figure 5. Synthetic edge: a) grey-level profile, b) response of MLR and SD edge operators compared.*

Figure 6. A total of 504 edge responses; 10-20 edge responses from over 35 test images were obtained.

Figure 6 shows a greater selectivity and improved localisation for the MLR operator. Figure 6(a) shows that the improved selectivity is maintained at all signal to noise ratios. Figures 6(b) and 6(c) show that the accuracy and precision of each operator is almost identical.

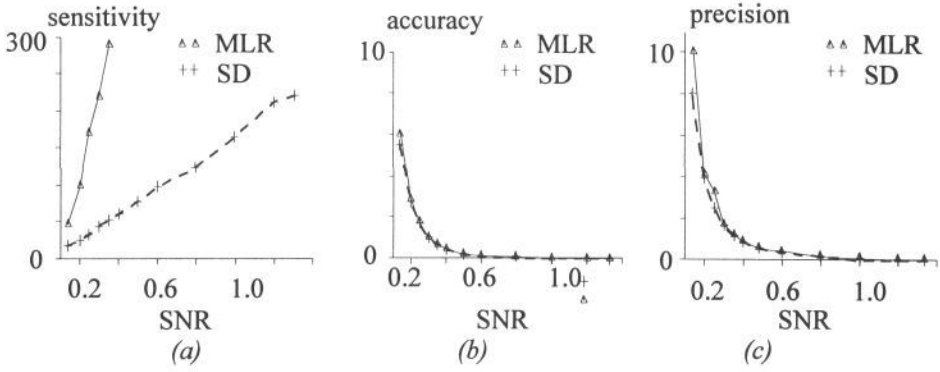


*Figure 6. Summary of Edge detection results for MLR and SD edge detection operator: a)sensitivity, b) accuracy and c)precision.*

4.2 Natural Image Data

Both operators were tested on a variety of images of epithelial cells at x60 magnification. Two typical images are shown in Figure 9 for their ability to locate the cytoplasm boundary of each cell. A point within the nucleus of each cell was manually selected as the origin for a set of radial search lines. A typical radial profile and the resulting edge response for the MLR and the SD operators are shown in Figure 7. This figure clearly shows that the magnitude of the edge step can be very small. The results show that the correct boundary points were identified with a high level of confidence more often by the MLR method than the SD method. The effectiveness of each edge detection method was evaluated using the relative magnitude of each response with respect to the response at the *true edge* position. Two measures $D_M$ and $D_N$ were used. $D_M$ is the difference between the response at the true edge position and the largest edge response. $D_N$ is the difference between the response at the true edge position and the magnitude of the nearest edge response The set of relative magnitudes in edge response for each profile were normalised over the range [-1, 1]. A histogram of the edge response difference for each of 209 profiles taken from a selection of cell images is shown in Figure 8. The ideal edge detector response is a maximum when $D_M$ and $D_N$ are 1.00 and zero elsewhere. Clearly the MLR method is significantly closer to achieving this than the standard deviation method.

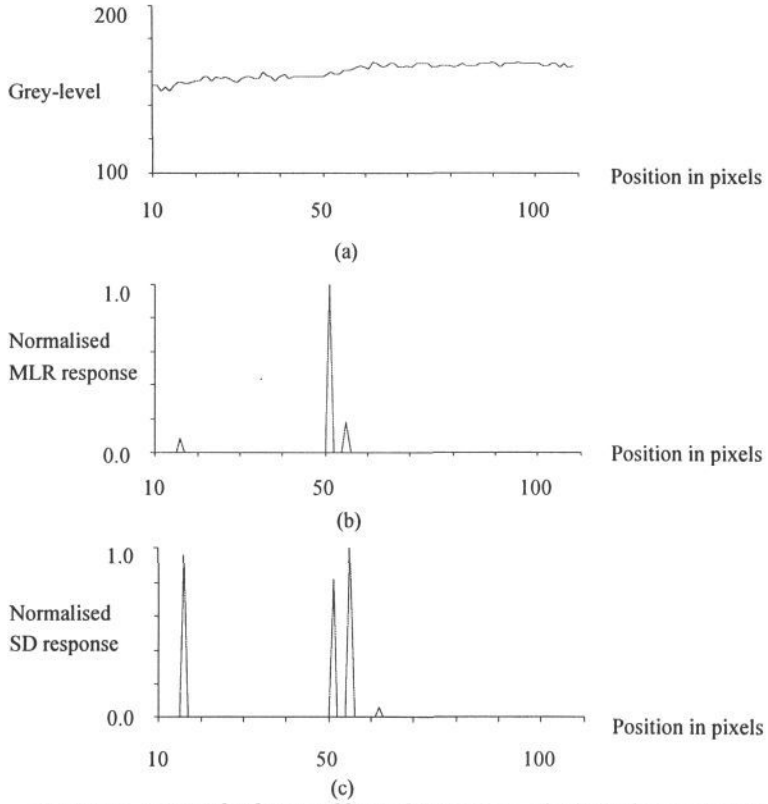


*Figure 7. Typical edge profile and response. a) Grey-level profile, b) Normalised MLR operator response, c) Normalised SD operator response.*

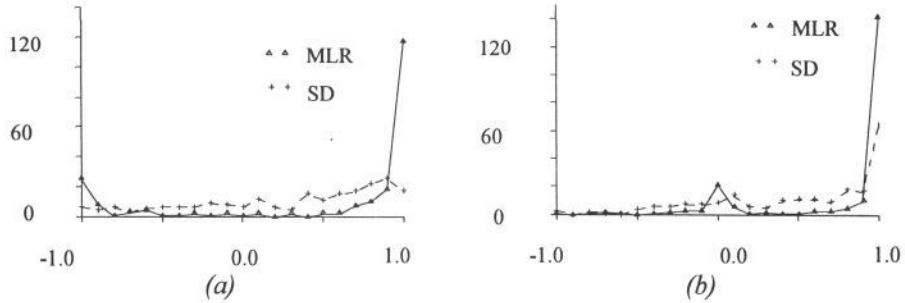


*Figure 8. Histogram of edge response for MLR and SD edge operators. a) Distance, $D_m$, between the position of the true edge and of the largest response; b) Distance, $D_n$, between the true edge position and the nearest detectable edge response.*

For the second experiment a consistent set of boundary points were selected by taking one point from the set along each radial search line. Candidate edge points along

each radial line were selected by taking the 8 points with the largest edge response. A consistent set of boundary points were then selected using dynamic programming and a linear combination of constraints that require a boundary to be compact and have a well defined edge[1]. The local maximum in the amplitude of the edge response in a linear combination and the local change in radial position was used to provide an indication of confidence in edge cue generation. In regions where the level of confidence in edge cue generation was low a series of circular searches were performed around the sparse sequence of boundary points with the result shown in Figure 9(b). Note the increased density of white dots and the reduced number of dark dots in Figure 9(b) as compared to Figure 9(a). In particular, in Figure 9(b), note the increased density of confident edge cue generation on the boundary of: the large cell at the top of the image; the large cell at the bottom; the elongated cell on the left near the bottom of the image; and the cell to the left of the image.

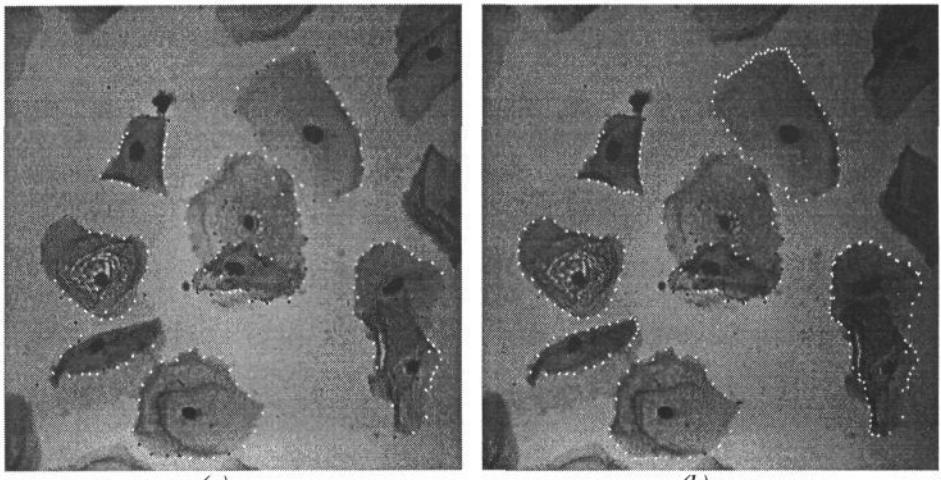

(a) (b)

*Figure 9. Boundary cue generation for free laying, touching and overlapping epithelial cells; a) Using a radial search strategy and b) Using an adaptive circular search strategy to improve cue generation.*

## 5. Conclusion

Statistical inference is used to interpret step, ramp and composite grey-level edges where an edge is modelled in terms of the grey-level distributions on each side of the edge. This approach provides a measure of confidence for each edge cue generated.

In this paper we have demonstrated the application of statistical inference and maximum likelihood criteria to provide a robust mechanism for generating grey-level edge cues. We have demonstrated that the resulting edge is more sensitive than other high sensitivity edge detectors[4], whilst preserving an equal degree of accuracy and precision. We have also demonstrated the benefit of an adaptive circular search path to improve the signal-to-noise ratio of edge profiles.

The cues generated using these techniques provide a good guide to the boundary of the cytoplasm of epithelial cells, which, in the images used have a very low grey-level

contrast and a complex grey-level edge profile (due to the close proximity and overlap of other cells).

This procedure was designed with a view to the interpretation of images of epithelial cells but it is suitable for application to a wide range of objects in 2-D images. Epithelial cells were chosen because they vary greatly in appearance whilst remaining relatively easy for people to recognise. Using the same edge detection strategy in a multi-model object interpretation system it is possible to achieve segmentation results that provide a similar precision to that achieved manually for cell images with a low grey-level contrast[7]. In that work on the segmentation of cell images an alternative strategy was adopted for selecting the orientation of the path used to locate the position of the grey-level edge.

## 5. References

[1] Azzopardi PJ, Pycock D, Taylor CJ and Wareham AC, "An experiment in Model-Based Boundary Detection", *in Proc. AVC88*, Manchester, 1988, pp31-36.

[2] Canny JF, "Finding lines and edges in images", MIT Artificial Intelligence Lab. Cambridge, MA, Tech. Rep. AI-TR-720, 1983.

[3] Duda RO and Hart PE, *Pattern Classification and Scene Analysis*, John Wiley & Sons, New York, 19783, pp 44-49.

[4] Graham J and Taylor CJ, "Boundary Cue Operators for Model-Based Image Processing", *in Proc. AVC88*, Manchester, 1988, pp 59-64.

[5] Huang JS and Tseng DH, "Statistical Theory of Edge Detection", Comp. Vis. Graphics and Image Proc., **43**, 1988, pp 337-346.

[6] Kundu A, "Robust Edge Detection", Pattern Recognition, **23**, 5, 1990, pp 423-440.

[7] P Zhou and Pycock D "Robust Statistical Model-Based Cell Image Interpretation", *Proc. BMVC'95*, Birmingham 1995.